Text S1- Methodology

Dataset

The Chandon 3D seismic reflection data have a bin spacing of 25 m and a record length of 6 seconds two-way time (s TWT). We use borehole velocity information to depth-convert the top 4 s TWT of the survey; beneath this level we lack sufficient borehole control and stacking velocity data for the survey to accurately estimate velocities. We present seismic images in which a trough (black) reflection corresponds to a downward increase in acoustic impedance whilst a peak (white) reflection represents a downward decrease in acoustic impedance (Fig. 2C).

Methods

We identify hanging wall and footwall cut-offs of each horizon along fault-perpendicular transects every 125 m along-strike. Where horizons are folded adjacent to the faults, which may reflect ductile strain, we project the regional trend of the strata to define cut-offs (Supplementary File 7) (Mansfield and Cartwright, 1996). For each cut-off pair, we measure fault throw and heave, from which we calculate fault dip and displacement (Supplementary File 7). We lack pre-kinematic piercing points (e.g., channels) to determine whether faulting was oblique- or dip-slip, so we assume displacement was dip-slip.

We measure graben half-width (HW), which corresponds to half the distance between EF1 and EF2, every 250 m along-strike on horizon HF (Supplementary File 7). These measurements were used with fault dip (α) to predict the depth to the dike upper tip (D') beneath horizon HF. We measured dike upper tip depths (D) beneath horizon HF every 250 m along-strike at the same location where HW was measured; dike thickness was measured from the RMS amplitude map (Fig. 1A) at the same spacing (Supplementary File 7).

Although horizon HF does not mark the top of the faults and thus does not represent their contemporaneous surface expression, testing whether D' is a realistic proxy for D can be conducted at any structural level within dike-induced graben. We selected horizon HF because it is the uppermost prominent reflection that both faults displace along their entire studied lengths.

Sources Of Error

There are several sources of error affecting confidence in quantitative measurements obtained from seismic reflection data. The primary error source in this study relates to seismic velocities used to convert the seismic data and measurements from depth in seconds two-way time (TWT) to depth in metres (Magee and Jackson, 2020). This uncertainty arises because seismic velocities are obtained from borehole data, which effectively only provide a 1D snapshots of the subsurface geology and may thus not capture lateral variations in rock properties and seismic velocity. The numerous wells in our study area all display similar time-depth relationships, which indicates seismic velocities remain relatively constant laterally (Supplementary Files 3 and 4). We thus take a conservative view that calculated seismic velocities and measured dominant frequencies vary by up to ±10% Supplementary Files 3 and 5). Measurements of limits of separability and visibility, fault cut-offs, fault dips, dike upper tip, and dike lower tip depths rely on depth-converting time data and are therefore considered to have errors of ±10%. The limits of separability and visibility refer, respectively, to the minimum vertical distance between two closely spaced or overlapping points or surfaces at which their separation can be: (i) accurately measured; and (ii) observed and differentiated from seismic noise. If the vertical distance between the two points or surfaces is below the limit of separability but above the limit of visibility, the energy they reflect convolves on its return to the surface and cannot be distinguished during processing; i.e. we

can be confident that the separation is real but the measured value may be inaccurate. We also acknowledge that manual mapping and measurement can introduce human errors; we cannot quantify these errors but conservatively assume they could be up to ±5%. Fault dip data were extracted by creating dip angle maps from depth-converted fault surfaces constructed using all footwall cut-offs mapped along HA–HK (~1500 per fault). The convergent interpolation gridding algorithm in Schlumbergers's Petrel seismic interpretation software was used to grid these data into a surface; this algorithm applies a linear projection to extrapolate between points and a 'trend' method to preserve data trends. Overall, data for graben half-width (*HW*) and dike width are presented with ±5% errors as they do not rely on depth-converting any measurements, whilst the dikes lower and upper tip depths (including *D* and *D'*), fault dips, displacement, and heave assume errors are ±15%. Fault displacement and dip maps may also contain interpolation errors derived from our choice gridding algorithms, but we consider these negligible given the high density of measurement locations across both faults.

References

Magee, C., and Jackson, C.-L., 2020, Seismic reflection data reveal the 3D structure of the newly discovered Exmouth Dyke Swarm, offshore NW Australia: Solid Earth, v. 11, no. 2, p. 576-606.

Mansfield, C. S., and Cartwright, J. A., 1996, High resolution fault displacement mapping from three-dimensional seismic data: evidence for dip linkage during fault growth: Journal of Structural Geology, v. 18, p. 14.
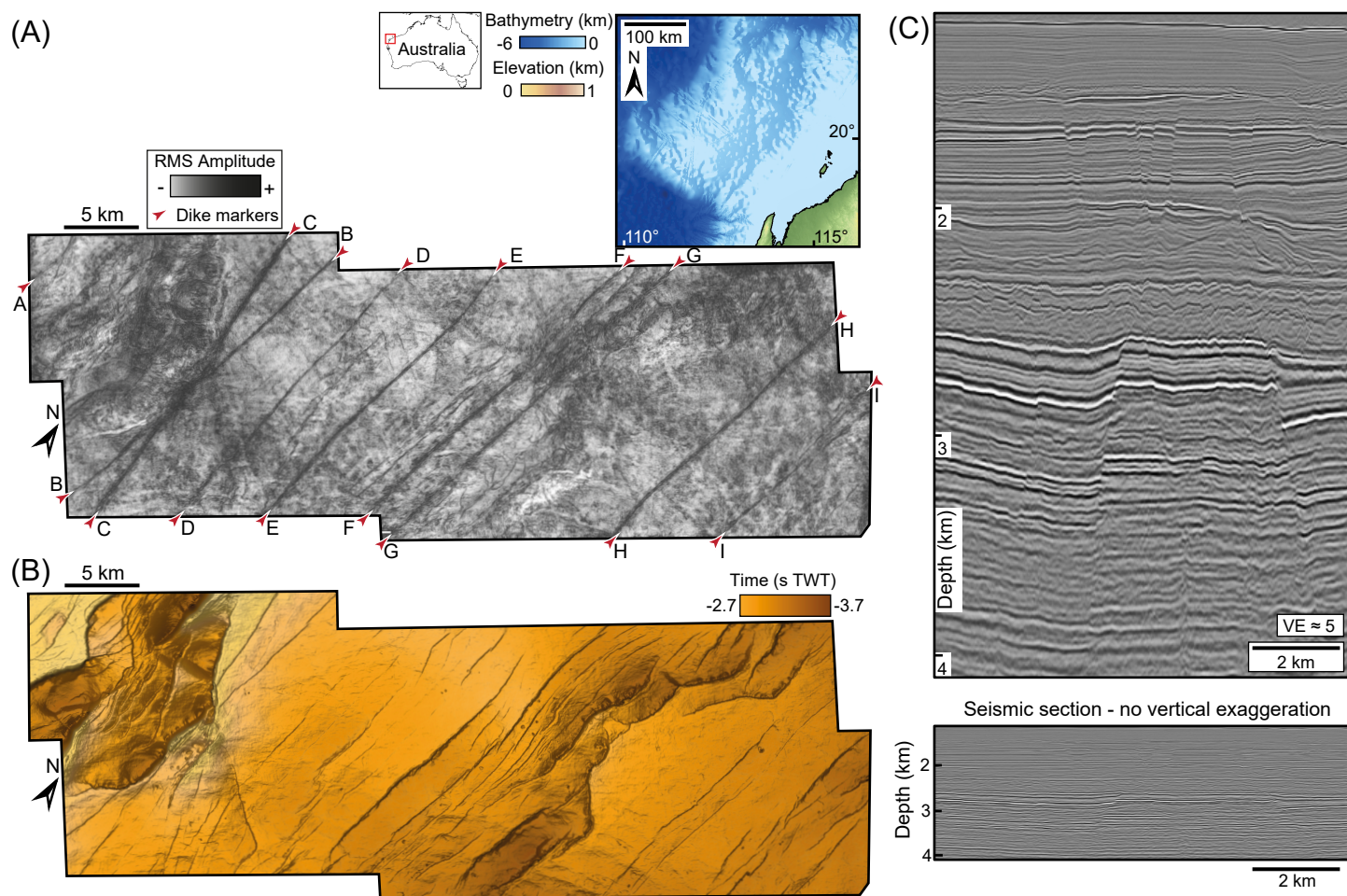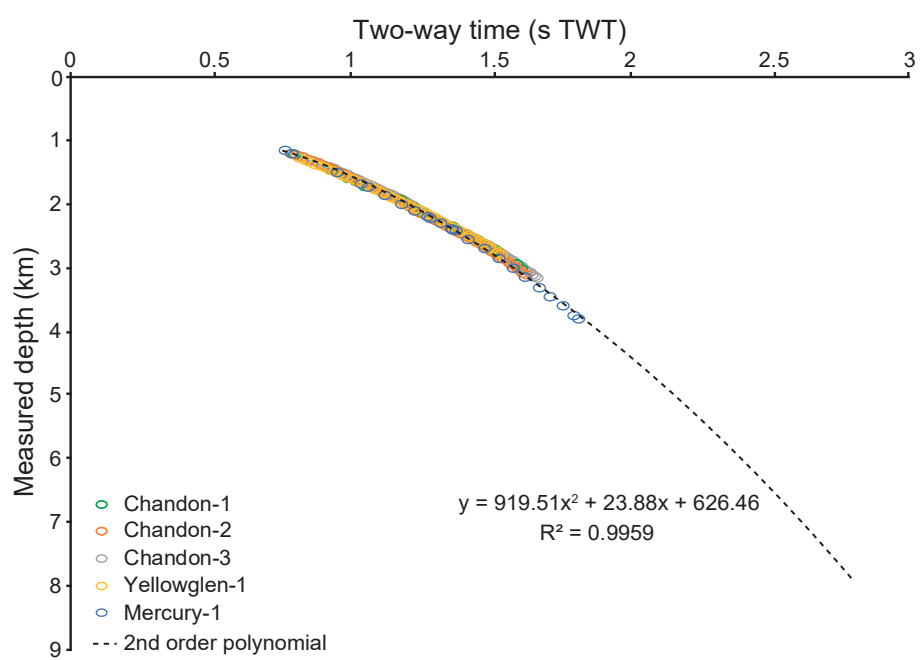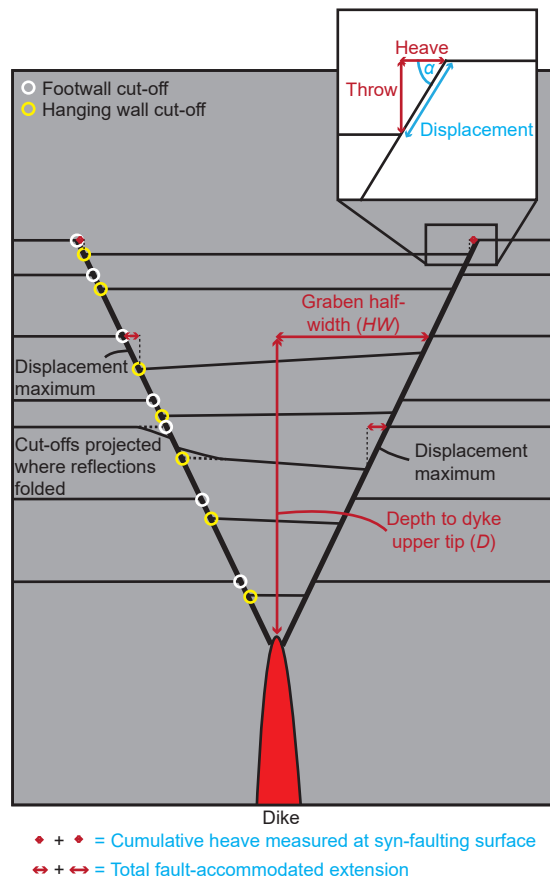
(A)

Australia

Bathymetry (km)
-6 ▮▮▮ 0

Elevation (km)
0 ▮▮▮ 1

100 km
N

20°

110°
115°

RMS Amplitude
- ▮▮▮ +
Dike markers

5 km

A
B
C
D
E
F
G
H
I

(B)

5 km
N

Time (s TWT)
-2.7 ▮▮▮ -3.7

(C)

2

3

Depth (km)

4

VE ≈ 5

2 km

Seismic section - no vertical exaggeration

2

Depth (km)

3

4

2 km

Figure S1

Figure S2

(A)

Footer labels: Footwall cut-off, Hanging wall cut-off, Heave, Throw, α, Displacement, Graben half-width (HW), Displacement maximum, Cut-offs projected where reflections folded, Displacement maximum, Depth to dyke upper tip (D), Dike

◆ + ◆ = Cumulative heave measured at syn-faulting surface

↔ + ↔ = Total fault-accommodated extension

(B)

5 km
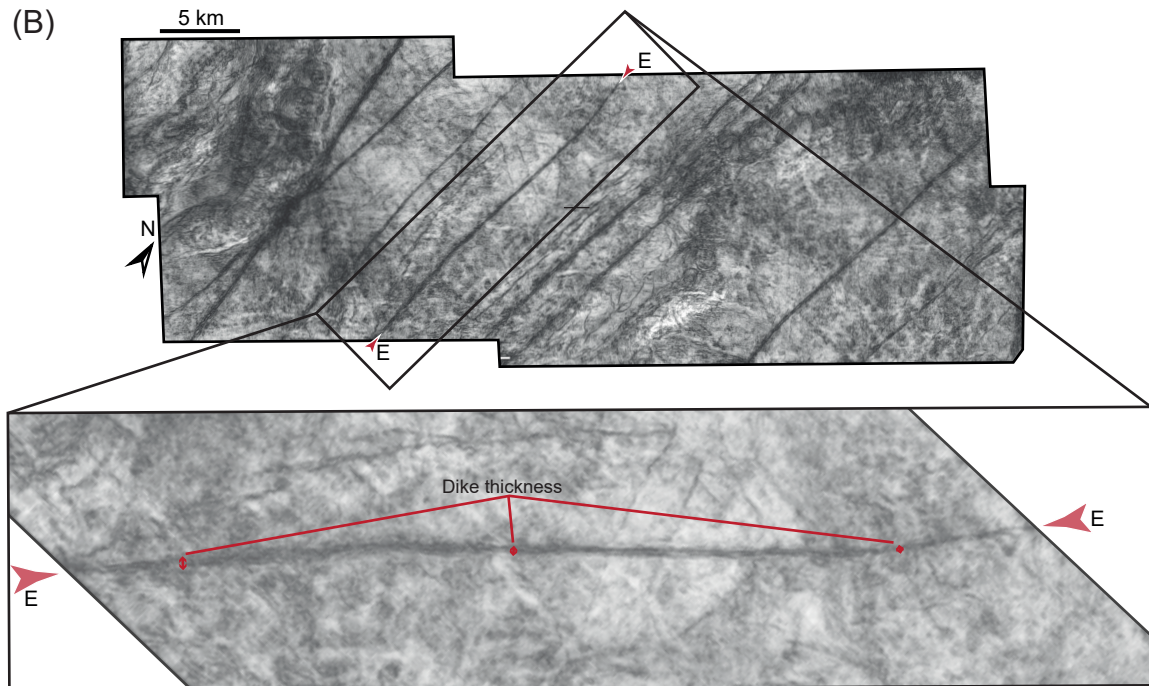
N

E

E

E

E

Dike thickness

Figure S3: (A) Cross-section schematic showing mapped elements (e.g., cut-offs), measured fault properties (red text and arrows), calculated fault properties (blue text and arrows). (B) Plan-view zoom-in showing the width of Dike E's seismic expression (i.e. orthogonal to margins), which is considered a proxy for dike thickness (see Figure 1A and Supplementary File 1).
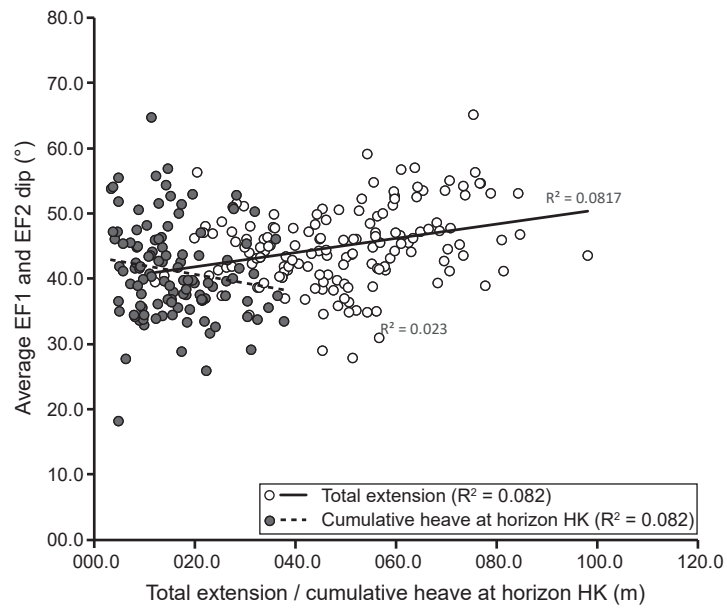
Figure S4: Cross-plot of total extension and cumulative heave (measured at horizon HK) against average fault dip of EF1 and EF2, showing there is no correlation.